Scientific Research Publishing

Advances in Materials Physics and Chemistry, 2024, 14, 113-122
https://www.scirp.org/journal/ampc
ISSN Online: 2162-5328
ISSN Print: 2162-531X

Study of the Magnetocaloric Effect in $La_{0.5}Sm_{0.2}Sr_{0.3}Mn_{1-x}Fe_xO_3$ (x = 0 and 0.05) Manganites with the Mean-Field Theory

Amnah Alofi, Salha Khadhraui

College of Science Physics Department, Al-Baha University, Al Baha, Saudi Arabia
Email: aalawfi@bu.edu.sa

How to cite this paper: Alofi, A. and Khadhraui, S. (2024) Study of the Magnetocaloric Effect in $La_{0.5}Sm_{0.2}Sr_{0.3}Mn_{1-x}Fe_xO_3$ (x = 0 and 0.05) Manganites with the Mean-Field Theory. *Advances in Materials Physics and Chemistry*, **14**, 113-122.
https://doi.org/10.4236/ampc.2024.147009

Received: June 1, 2024
Accepted: July 27, 2024
Published: July 30, 2024

Copyright © 2024 by author(s) and Scientific Research Publishing Inc.
This work is licensed under the Creative Commons Attribution International License (CC BY 4.0).
http://creativecommons.org/licenses/by/4.0/

Open Access

Abstract

In this paper, the magnetocaloric in $La_{0.5}Sm_{0.2}Sr_{0.3}Mn_{1-x}Fe_xO_3$ compounds with x = 0 (LSSMO) and x = 0.05 (LSSMFO) were simulated using mean field model theory. A strong consistency was observed between the theoretical and experimental curves of magnetizations and magnetic entropy changes, $-\Delta S_M(T)$. Based on the mean-field generated $-\Delta S_M(T)$, the substantial Temperature-averaged Entropy Change (TEC) values reinforce the appropriateness of these materials for use in magnetic refrigeration technology within TEC (10) values of 1 and 0.57 $J \cdot kg^{-1} \cdot K^{-1}$ under 1 T applied magnetic field.

Keywords

Manganites, Magnetization, Magnetocaloric Effect, Mean Field Model, Simulation

1. Introduction

Magnetic refrigeration is gaining increasing attention due to its potential to address environmental concerns and energy efficiency in refrigeration technology. The necessity for magnetic refrigeration arises from the limitations and environmental impact of conventional refrigeration methods, particularly those based on vapor compression cycles and refrigerants with high global warming potential [1]-[3]. Conventional refrigeration systems contribute significantly to greenhouse gas emissions through the use of hydrofluorocarbon refrigerants, which are known contributors to climate change. Additionally, these systems often suffer from energy inefficiency and require periodic maintenance, leading to increased operating costs [4]-[6]. Magnetic refrigeration offers a sustainable alternative by utilizing the magnetocaloric effect (MCE) in certain materials,

which allows for efficient and environmentally friendly cooling without the need for harmful refrigerants. This technology has the potential to significantly reduce energy consumption and greenhouse gas emissions in various applications, including household refrigerators, air conditioning systems, and industrial cooling processes [7]-[9].

The modelling of the MCE plays a crucial role in advancing the understanding and optimization of magnetocaloric materials for various applications. By simulating the behavior of MCE materials under different magnetic fields, temperatures, and compositions, researchers can predict their thermodynamic properties and performance characteristics with high precision [10]. This predictive capability is essential for designing efficient magnetocaloric cooling systems and optimizing their energy efficiency. Furthermore, simulations enable researchers to explore the underlying mechanisms governing the MCE, such as magnetic phase transitions and lattice dynamics, providing valuable insights into the material's behavior at the atomic and molecular levels [11]. Additionally, they allow for the rapid screening of potential magnetocaloric candidates, accelerating the discovery of novel materials with enhanced refrigeration capabilities and reduced environmental impact. Moreover, simulation-based approaches facilitate the design of tailored magnetic structures and configurations to optimize the magnetocaloric response, leading to the development of more compact and cost-effective cooling devices. Overall, they are indispensable tools for advancing the field of magnetic refrigeration and realizing its full potential in addressing global energy and environmental challenges.

Particularly, the mean-field model serves as a powerful tool in simulating MCE, offering insights into the thermodynamic behavior of magnetocaloric materials under varying magnetic fields [12]-[14]. In this model, the magnetic interactions within the material are approximated by a mean field, simplifying the complex interactions between individual magnetic moments. By employing the mean-field approach, researchers can predict key thermodynamic properties such as the magnetic entropy change and adiabatic temperature change, which are crucial for evaluating the cooling performance of magnetocaloric materials [15]. Additionally, this model allows for the investigation of phase transitions and critical phenomena associated with the MCE, shedding light on the underlying physics governing these processes [16]. Recent advancements in computational techniques have further enhanced the accuracy and applicability of mean-field simulations, enabling researchers to explore a wide range of magnetocaloric materials and operating conditions [17]. These simulations have contributed to the discovery of novel magnetocaloric compounds and the optimization of existing materials for practical cooling applications [18]. Moreover, mean-field modelling provides valuable guidance for the design and engineering of magnetocaloric devices with enhanced efficiency and reliability, driving forward the development of next-generation magnetic refrigeration technologies. In applications way, manganites play a crucial role in the MCE due to their

unique magnetic and structural properties [19]. These materials undergo a magnetostructural transition, leading to significant changes in entropy under the influence of a magnetic field, making them ideal candidates for magnetic refrigeration. Recent studies have investigated the MCE in various manganite compounds, highlighting their potential for efficient cooling applications [20] [21].

In this work we will apply the mean-field theory to model the MCE in $La_{0.5}Sm_{0.2}Sr_{0.3}Mn_{1-x}Fe_xO_3$ compounds with $x = 0$ (LSSMO) and $x = 0.05$ (LSSMFO). In their work, Khouloud *et al.* [22] investigated the structural, magnetic, and magnetocaloric properties of $La_{0.5}Sm_{0.2}Sr_{0.3}Mn_{1-x}Fe_xO_3$ compounds within the range of x from 0 to 0.05. X-ray diffraction analysis reveals the compounds maintain a rhombohedral structure throughout the studied range of x. The substitution of Fe for Mn induces a decrease in the magnetic moment and Curie temperature with increasing Fe content. The compounds exhibit significant magnetocaloric effects, characterized by the maximum magnetic entropy change, which decreases with increasing Fe content.

2. Results and Discussions

The Brillouin function, $B_J(x)$, is commonly used to describe the magnetization M behavior of a ferromagnetic material at finite temperatures T and applied fields H:

$$M(H,T) = M_0 B_J(x) \tag{1}$$

Where: M_0 is the saturation magnetization,

$$B_J(x) = \frac{2J+1}{2J}\coth\left(\frac{2J+1}{2J}\frac{Jg\mu_B}{k_B}\left(\frac{H+H_{exch}}{T}\right)\right) - \frac{1}{2J}\coth\left(\frac{1}{2J}\frac{Jg\mu_B}{k_B}\left(\frac{H+H_{exch}}{T}\right)\right)$$

with $x = \frac{Jg\mu_B}{k_B}\left(\frac{H+H_{exch}}{T}\right)$, $H_{exch} = \lambda M$ [23] is the exchange magnetic with λ is the exchange parameter, J is the total angular momentum, g the Lande factor, μ_B is the Bohr magnetron and k_B is the Boltzmann.

By incorporating the expression $M(T,H) = f\left(\frac{H+H_{exch}}{T}\right)$ and utilizing the inverse function f^{-1} of f, we derive the following relationship:

$$\frac{H}{T} = f^{-1}(M) - \frac{H_{exch}}{T} \tag{2}$$

The magnetic entropy can be expressed by Maxwell relations as $\left(\frac{\partial S}{\partial H}\right)_T = \left(\frac{\partial M}{\partial T}\right)_H$ or $\left(\frac{\partial S}{\partial M}\right)_T = -\left(\frac{\partial H}{\partial T}\right)_M$. Consequently, between two magnetic fields H_1 and H_2, the magnetic entropy change is given by:

$$-\Delta S_M(T) = \int_{M|_{H_1}}^{M|_{H_2}} \left(f^{-1}(M) - \left(\frac{\partial \lambda(T)}{\partial T}\right)_M M \right) \mathrm{d}M \tag{3}$$

The isotherms $M(H,T)$ of the LSSMO and LSSMFO compounds were

analyzed, and the evolution of $\frac{H}{T}$ versus $\frac{1}{T}$ at constant magnetization values was plotted in Figure 1. A linear relationship of the plots was observed, with isomagnetics curves shifting towards higher temperature values. Linear fits were applied to these curves to determine the exchange mean-field parameter, obtained from the slopes representing H_{exch}.

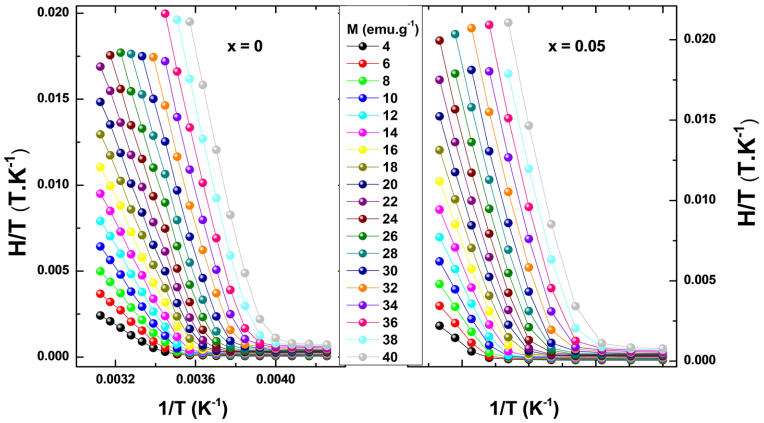

Figure 1. $\frac{H}{T}$ vs. $\frac{1}{T}$ with at various magnetizations.

In the paramagnetic domain or materials with ordered domains like antiferromagnetic, the expansion of M in powers of H or H in powers of M was performed up to the third order, considering the magnetization as an odd function of the field: $H_{exch} = \lambda_1 M + \lambda_3 M^3$.

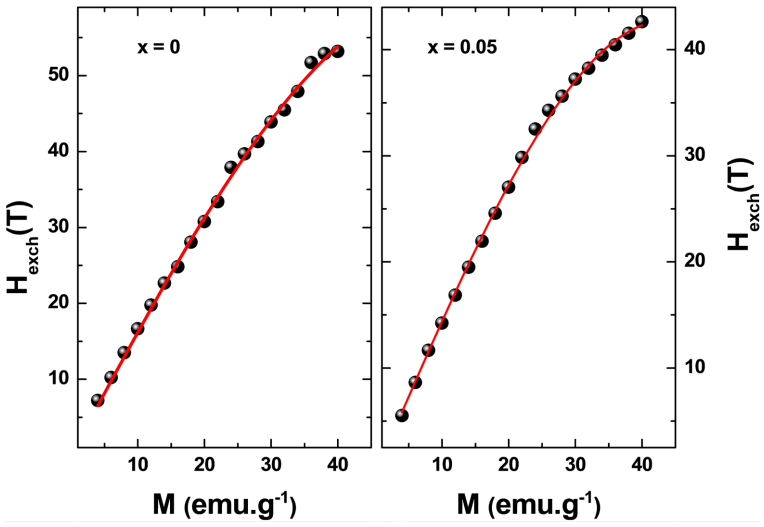

Figure 2. Fitting H_{exch} vs M with the equation: $H_{exch} = \lambda_1 M + \lambda_3 M^3$.

Then, the adjustment of H_{exch} versus M in Figure 2 is carried out. It has been observed a very small dependence on M^3 which could be negligeable and only λ_1 may be kept. Thus $H_{exch} = \lambda_1 M \approx \lambda M$, with $\lambda = 1.63$ and 1.46 T.emu^{-1}.g for LSSMO and LSSMFO samples, respectively.

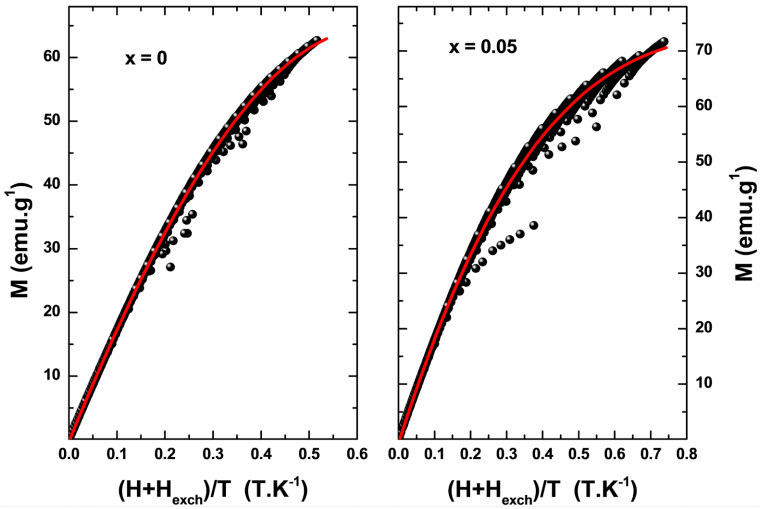

Figure 3. Fitting M vs. $\frac{H+H_{exch}}{T}$ with the equation: $M(H,T)=M_0 B_J(x)$.

The next step of this approach involves constructing a scaling plot of M vs. $\frac{H+H_{exch}}{T}$, as depicted in **Figure 3** with black symbols. Essentially, these curves, converging into a single curve, are fitted with Equation (1) to ascertain M_0, J, and g. **Figure 3** displays certain data points that noticeably deviate from the scaling function. These points correspond to the magnetic domain region, characterized by low fields and temperatures below the Curie temperature. The different adjusted parameters of the LSSMO and LSSMFO are summarized in **Table 1**.

Table 1. Different adjusted parameters of the LSSMO and LSSMFO compounds.

Sample	M_0 (emu.g^{-1})	J	g
LSSMO	82.65	1.98	2.61
LSSMFO	83.15	2	3.53

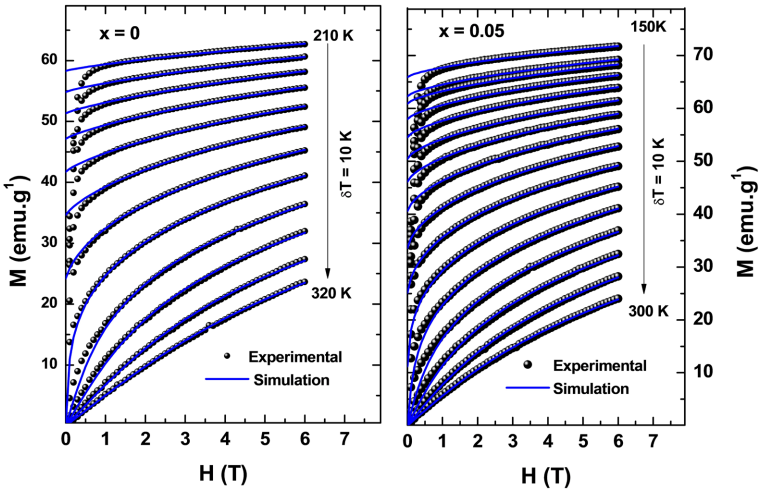

Figure 4. Comparison between experimental (black symbols) and generated (blue lines) $M(H,T)$ curves using the mean-field model.

The numerical resolution of Equation (1) with the given adjusted parameters λ, J, g and M_0 has been achieved using MATLAB software. Generated (blue lines) and experimental (black symbols) isotherms $M(H,T)$ are correlated as depicted in Figure 4.

Figure 5 illustrates the comparison between the mean-field generated $-\Delta S_M(T)$ curves (red lines) obtained using Equation (3) and the corresponding experimental results (solid symbols) obtained using the Maxwell relation. A clear agreement is observed between the generated and experimental $-\Delta S_M(T)$ curves.

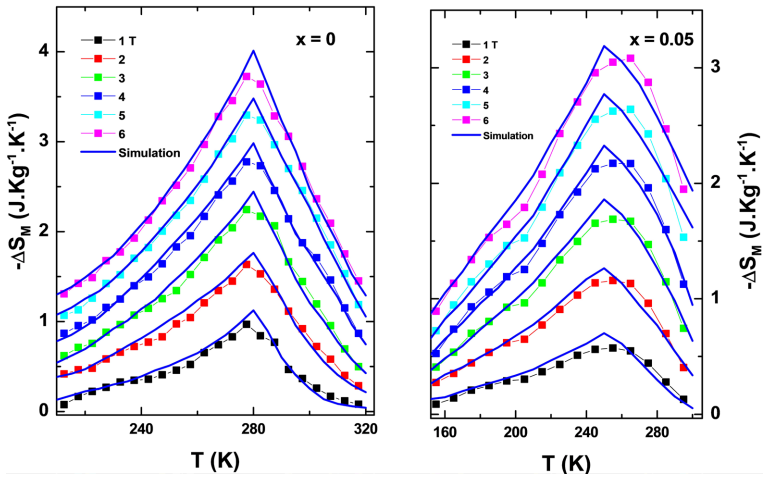

Figure 5. Comparison between experimental (symbols) and simulated (blue lines) $-\Delta S_M(T)$ curves using the mean-field model.

In fact, the applicability of Maxwell relation may be limited in complex systems where deviations from ideal behavior occur, such as in strongly correlated electron systems or systems with competing magnetic interactions. On the other hand, the mean-field model is a simplified theoretical approach that approximates the behavior of a system by assuming that each magnetic moment interacts with an effective average field. This model is often more tractable and can provide reasonable estimates of magnetic properties in many cases, especially for systems where interactions between magnetic moments are relatively weak and can be treated perturbatively. However, it may fail to capture the effects of fluctuations and correlations that are important in strongly interacting systems.

To assess the efficiency of a refrigerant substance, a proposed metric known as the Temperature-averaged Entropy Change (TEC) is suggested [24] [25]:

$$\mathrm{TEC} = \frac{1}{\Delta T_{H-C}} \max\left\{ \int_{T_{mid}-\frac{\Delta T_{H-C}}{2}}^{T_{mid}+\frac{\Delta T_{H-C}}{2}} \left|\Delta S_M\right| \mathrm{d}T \right\} \tag{4}$$

Where ΔT_{H-C} represents the specified range of temperatures(in this study $\Delta T_{H-C} = 2,5$ and 10 K) and T_{mid} is the temperature maximizing the integration.

TEC is based on the temperature range within which the material is designed

or capable of delivering the maximum isothermal entropy change. This metric aims to quantify the magnitude of the thermodynamic effect across a practical temperature spectrum, thereby indicating the material's effectiveness in practical applications. Greater performance is achieved with larger TECs at wider ΔT_{H-C} ranges. Figure 6 illustrates the change in TECs as the field changes for various ΔT_{H-C} values. The values decrease as the temperature span ΔT_{H-C} increases across all samples.

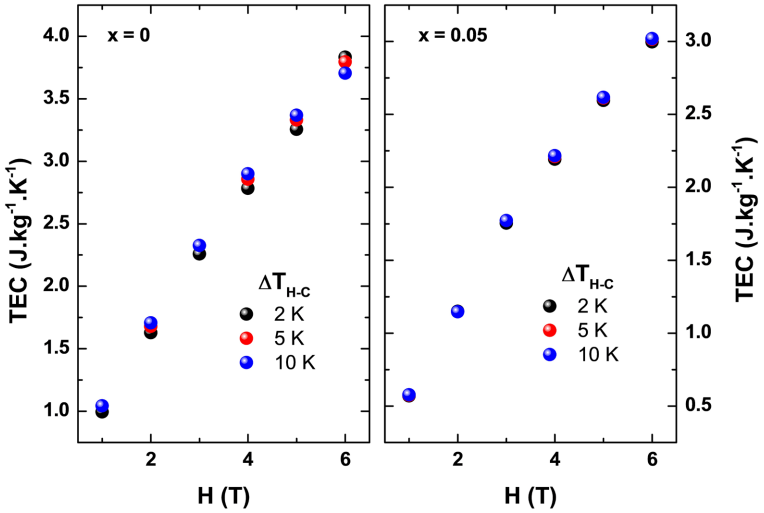

Figure 6. The magnetic field dependence of the temperature-averaged entropy change at different ΔT_{H-C}.

The data in Figure 6 shows that TEC values stabilize across different ΔT_{H-C} (2 K, 5 K, 10 K) as the magnetic field changes, indicating that the magnetic field strength, rather than temperature differences, primarily influences TEC. This stabilization suggests that once the magnetic field reaches a certain strength, its effect on entropy change dominates, becoming less dependent on temperature variations. This phenomenon likely arises from the material's intrinsic properties, with the magnetic field inducing a state where entropy change due to magnetic effects is predominant. At higher magnetic fields, the TEC values plateau, indicating a saturation effect where further increases in the magnetic field do not significantly alter TEC, making the material less sensitive to temperature differences. The significant TEC values obtained further bolster the suitability of these materials for application in magnetic refrigeration technology. Under 1 T field, TEC(10) = 1 and 0.57 $J.kg^{-1}.K^{-1}$ for the LSSMO and LSSMFO compounds, respectively. These values are near to the ones of Gd (2.91 $J.kg^{-1}.K^{-1}$) [26].

3. Conclusion

In conclusion, isotherms $M(H,T)$ of LSSMO and LSSMFO compounds, were analyzed. the linear fits of $\frac{H}{T}$ versus $\frac{1}{T}$ at constant magnetization determine the exchange mean-field H_{exch}, which is approximated as λM. A scaling plot

of M versus $\frac{H+H_{exch}}{T}$ is constructed and fitted to sort out the total angular momentum J, the Lande factor, g and the saturation magnetization M_0. The comparison between mean-field generated isotherms $M(H,T)$ and magnetic entropy change $-\Delta S_M(T)$ curves with experimental results show a strong agreement. A proposed metric, Temperature-averaged Entropy Change (TEC), indicates the materials' effectiveness in practical applications. The change in TECs with varying fields and specified range of temperatures ΔT_{H-C} values further support the materials' suitability for magnetic refrigeration technology.

Acknowledgements

Experimental data were kindly provided by Abdouli K.

Conflicts of Interest

The author declares no conflicts of interest regarding the publication of this paper.

References

[1] Li, L.W. and Mi, Y. (2023) Recent Progress in the Development of $Re_2TMTM'O_6$ Double Perovskite Oxides for Cryogenic Magnetic Refrigeration. *Journal of Materials Science & Technology*, **136**, 1-12. https://doi.org/10.1016/j.jmst.2022.01.041

[2] Wang, Q.W., Wu, Q., Cheng, H.F., *et al.* (2023) Review of the Research on Oxides in Low-Temperature Magnetic Refrigeration. *Journal of the European Ceramic Society*, **43**, 6665-6680. https://doi.org/10.1016/j.jeurceramsoc.2023.07.063

[3] Hojat, A., Fatimah, M. and Khojasteh-Salkuyeh, Y. (2023) Conceptual Design of Two Novel Hydrogen Liquefaction Processes Using a Multistage Active Magnetic Refrigeration System. *Applied Thermal Engineering*, **230**, Article 120771. https://doi.org/10.1016/j.applthermaleng.2023.120771

[4] Lee, J.S. (2023) Thermodynamic Analysis on a Magnetic Refrigeration System. *International Journal of Air-Conditioning and Refrigeration*, **31**, Article No. 23. https://doi.org/10.1007/s44189-023-00040-w

[5] Souheila, M. (2023) Introduction to Magnetic Refrigeration: Magnetocaloric Materials. *International Journal of Air-Conditioning and Refrigeration*, **31**, Article No. 5. https://doi.org/10.1007/s44189-023-00021-z

[6] Gao, L., Wang, P.Y., *et al.* (2023) Performance Study of a Double-Regenerator Room Temperature Magnetic Refrigerator with 26˚C Temperature Span. *International Journal of Refrigeration*, **148**, 143-151. https://doi.org/10.1016/j.ijrefrig.2023.01.007

[7] Ali Osman, A., Çetin, S.K., *et al.* (2023) Magnetic Refrigeration: Current Progress in Magnetocaloric Properties of Perovskite Manganite Materials. *Materials Today Communications*, Article 105988. https://doi.org/10.1016/j.mtcomm.2023.105988

[8] Suye, B., Yibole, H., Meijuan, W., Wurentuya, B. and Guillou, F. (2023) Influence of the Particle Size on a MnFe (P, Si, B) Compound with Giant Magnetocaloric Effect. *AIP Advances*, **13**, Article 025203. https://doi.org/10.1063/9.0000371

[9] Liu, Z.W. (2023) Advances in Metal-Containing Magnetic Materials and Magnetic Technologies. *Metals*, **13**, Article 1318. https://doi.org/10.3390/met13071318

[10] Souhir, B., Hsini, M., *et al.* (2023) Magnetocaloric Effect and Critical Behavior of the $La_{0.75}Ca_{0.1}Na_{0.15}MnO_3$ Compound. *RSC Advances*, **13**, 16529-16535. https://doi.org/10.1039/D3RA02443A

[11] Nawel, K., Salha, K. and Hsini, M. (2023) Critical Behaviour and Magnetocaloric Effect Simulation in Tb_2Rh_3Ge. *Bulletin of Materials Science*, **46**, Article No. 221. https://doi.org/10.1007/s12034-023-03056-5

[12] Starkov, I.A. and Starkov, A.S. (2023) Modeling of the Magnetobarocaloric Effect in the Framework of the Mean-Field Theory. *Journal of Magnetism and Magnetic Materials*, **587**, Article 171344. https://doi.org/10.1016/j.jmmm.2023.171344

[13] Caro, P.J. and de Oliveira, N.A. (2023) Magnetocaloric Effect in R_2Cu_2Cd (R=Gd, Tb, Er, Tm). *Physica B*: *Condensed Matter*, **650**, Article 414496. https://doi.org/10.1016/j.physb.2022.414496

[14] Abassi, M., Zaidi, N. and Hlil, E.K. (2023) Magnetocaloric Effect Simulation in TbFeSi and DyFeSi Intermetallic Magnetic Alloys Using Mean-Field Model. *Journal of Superconductivity and Novel Magnetism*, **36**, 397-401. https://doi.org/10.1007/s10948-022-06490-4

[15] Pérez, E. and Rodríguez, M. (2022) Mean-Field Simulations of Magnetocaloric Materials under Non-Equilibrium Conditions: Implications for Rapid Cooling Applications. *Journal of Thermal Analysis and Calorimetry*, **143**, 1991-2001.

[16] Mohamed, H., Hcini, S. and Zemni, S. (2018) Magnetocaloric Effect Studying by Means of Theoretical Models in $Pr_{0.}5Sr_{0.5}MnO_3$ Manganite. *Journal of Magnetism and Magnetic Materials*, **466**, 368-375. https://doi.org/10.1016/j.jmmm.2018.07.051

[17] Mohamed, H., Hcini, S. and Zemni, S. (2019) Magnetocaloric Effect Simulation by Landau Theory and Mean-Field Approximation in $Pr_{0.5}Sr_{0.5}MnO_3$. *The European Physical Journal Plus*, **134**, Article No. 588. https://doi.org/10.1140/epjp/i2019-12975-4

[18] Mohamed, H. and Boutaleb, M. (2020) Simulation of the Magnetocaloric Effect by Means of Theoretical Models in Gd_3Ni_2 and Gd_3CoNi Systems. *The European Physical Journal Plus*, **135**, Article No. 186. https://doi.org/10.1140/epjp/s13360-020-00105-4

[19] Sudharshan, V., Munendra Pal, T.D.R. and Asthana, S. (2024) Investigation of Magnetocaloric Effect and Critical Field Analysis of $Nd_{0.7}$-XLax$Sr_{0.3}MnO_3$ (X= 0.0 - 0.3) Manganites. *ECS Journal of Solid State Science and Technology*, **13**, Article 043016. https://doi.org/10.1149/2162-8777/ad3fe7

[20] Xie, Z.J., Feng, M., Zou, Z.G., Jiang, X.Y. and Zhang, W.J. (2023) Structural, Magnetic, and Magnetocaloric Properties of $La_{0.67}Sr_{0.33}$-XKx$Mn_{0.95}Ni_{0.05}O_3$ Manganites (X= 0.10, 0.125, and 0.15): A-Site Doping. *Journal of Superconductivity and Novel Magnetism*, **36**, 1751-1766. https://doi.org/10.1007/s10948-023-06617-1

[21] Pan, B.L., Luo, X.Y., Fang, J.Y., Wu, Q., Yu, N.J., *et al.* (2023) Structural, Magnetic and Magnetocaloric Investigation of $La_{0.7}$-X Eu X $Ba_{0.3}MnO_3$ Manganites. *Bulletin of Materials Science*, **46**, Article No. 59. https://doi.org/10.1007/s12034-022-02882-3

[22] Kh, A., Cherif, W., *et al.* (2019) Structural, Magnetic and Magnetocaloric Properties of $La_{0.5}Sm_{0.2}Sr_{0.3}$Mn1-XFe_XO_3 Compounds with (0≤ X≤ 0.15). *Journal of Magnetism and Magnetic Materials*, **475**, 635-642. https://doi.org/10.1016/j.jmmm.2018.12.007

[23] Charles, K. and McEuen, P. (2018) Introduction to Solid State Physics. Wiley.

[24] Liu, Q.Y., Wang, J.F., Xie, H.C., Fu, Q., *et al.* (2023) Giant Low-Field Magnetocaloric Effect in Hexagonal $Eu_3B_2O_6$ Compound. *Journal of Alloys and Compounds*, **936**, Article 168372. https://doi.org/10.1016/j.jallcom.2022.168372

[25] Shu, Y.Y., Wang, L.F., Huang, S.L. and Zhang, Y.K. (2024) Magnetic Properties and

Large Magneto-Caloric Effect in the Amorphous $Ho_{0.2}Tm_{0.2}Gd_{0.2}Co_{0.2}Al_{0.2}$ Ribbons. *Journal of Non-Crystalline Solids*, **628**, Article 122846. https://doi.org/10.1016/j.jnoncrysol.2024.122846

[26] Pramod, N., Murari, R.M.S. and Daivajna, M.D. (2024) Influence of Heat Sintering on the Physical Properties of Bulk La 0.67 Ca 0.33 MnO_3 Perovskite Manganite: Role of Oxygen in Tuning the Magnetocaloric Response. *Physical Chemistry Chemical Physics*, **26**, 5237-5252. https://doi.org/10.1039/D3CP04185A